



Published in final edited form as:

*Curr Eye Res.* 2010 June ; 35(6): 510–518. doi:10.3109/02713681003597255.

## Metabolic Responses to Light in Monkey Photoreceptors

Shufan Wang<sup>1</sup>, Gülnur Birol<sup>1</sup>, Ewa Budzynski<sup>1</sup>, Robert Flynn<sup>1</sup>, and Robert A. Linsenmeier<sup>1,2,3</sup>

<sup>1</sup> Department of Biomedical Engineering, Northwestern University, Evanston and Chicago, IL

<sup>2</sup> Department of Neurobiology & Physiology, Northwestern University, Evanston and Chicago, IL

<sup>3</sup> Department of Ophthalmology, Northwestern University, Evanston and Chicago, IL

### Abstract

**Purpose**—Transient changes in intraretinal oxygen tension ( $PO_2$ ) in response to light stimuli were studied in order to understand the dynamics of light-evoked changes in photoreceptor oxidative metabolism.

**Methods**— $PO_2$  changes during illumination were recorded by double-barreled microelectrodes in the outer part of the perifoveal retina in five macaques (Rhesus and Cynomolgus), and were fitted to a single exponential equation to obtain the time constant ( $\tau$ ) and maximum  $PO_2$  change.

**Results**—At the onset of light,  $PO_2$  increased at all illuminations in all animals. The magnitude of the light-evoked  $PO_2$  change increased with increasing illumination over 3–4 log units, but decreased in all animals at the maximum illumination. The median time constant of the  $PO_2$  change ( $\tau$ ) was 26 seconds and was not correlated with illumination. The time constant for the return to darkness was similar for illuminations below rod saturation. Since  $O_2$  diffusion is fast over the short distance from the choroid to the inner segments,  $\tau$  reflects the time course of the underlying change in oxidative metabolism.

**Conclusions**—Previous results suggested that two competing processes influence the change in photoreceptor oxidative metabolism with light,  $Na^+/K^+$  pumping and cGMP turnover. Because a single exponential fitted the  $PO_2$  data, it appears that these processes have time constants that differ by no more than a few seconds in primate. In monkeys,  $\tau$  is longer than previously reported values for cat and rat. Longer time constants are related to larger photoreceptor volume, possibly because metabolic rate is controlled by intracellular  $Na^+$ , and a change in intracellular  $Na^+$  after the onset of illumination occurs more slowly in larger photoreceptors. The “metabolic threshold” illumination that reduced oxygen consumption by about 10% is approximately the same as the illumination that closes 10% of the light-dependent cation channels that are open in the dark.

### Keywords

non-human primate; monkey; retinal metabolism; photoreceptor; retina; oxygen; macaque

### Introduction

It has been recognized for many years that light decreases photoreceptor metabolism [1,2]. One way to observe this is to record  $PO_2$  in the outer half of the retina, where, under normal physiological conditions,  $PO_2$  increases at the onset of light [3]. Because the choroidal  $PO_2$

Correspondence: Robert A. Linsenmeier, Biomedical Engineering Department, Northwestern University, 2145 Sheridan Road, Evanston, IL 60208-3107, Phone: (847) 491-3043, Fax: (847) 491-4928, r-linsenmeier@northwestern.edu.

No author has any conflict of interest or financial interest in this work.

and inner retinal  $PO_2$  at the boundaries of the photoreceptor are affected little if at all by light [4,5], the increase in  $PO_2$  can be interpreted as a decrease in photoreceptor oxygen consumption ( $QO_2$ ). Most of the information on this metabolic change has compared only darkness and strong steady illumination. Only two studies, in cat [3] and toad [6] retina, have characterized the dependence of photoreceptor oxidative metabolism on illumination, and neither attempted to compare the illumination required for a metabolic change to that required for other light-dependent retinal processes.

The observed decrease in  $QO_2$  is the result of two light-dependent processes. The first is a decrease in the demand for  $Na^+$  pumping in the photoreceptor inner segments [7] when the outer segment cation channels close and intracellular  $Na^+$  decreases. This process decreases the workload of the  $Na^+/K^+$  pump, and thus decreases  $QO_2$ . When the  $Na^+$  pump was inhibited by lowering the extracellular  $Na^+$  concentration or poisoning the pump,  $QO_2$  increased during illumination [6,8,9]. The process that increases  $QO_2$  is due to increased GTP utilization for cGMP turnover in the light [6,8,10]. This second process could be blocked with IBMX in toad retina, which decreased the rate of cGMP turnover, and under that condition, no light-dependent metabolic processes remained [6].

The dynamics of the light-dependent metabolic change have been studied by recording  $PO_2$  changes at the onset of light with intraretinal microelectrodes in intact cat [11] and rat [12] retina and isolated toad retina [6]. The  $PO_2$  changes could be fitted with a single or double exponential model. In the cat, a single exponential model was adequate, suggesting that the light-evoked changes in both  $Na^+$  pumping and cGMP turnover had similar rates [11]. However, a double exponential model with two time constants was required in the toad, with the time constant of cGMP turnover (increasing  $QO_2$ ; decreasing  $PO_2$ ) being faster than the time constant for the change in  $Na^+$  pumping [6].

In this work we investigated the time course of light-evoked  $PO_2$  changes in the photoreceptors of the rod-dominated perifoveal retina of macaques. We were interested in the dependence of  $QO_2$  on illumination and how this compared to the illumination required for other light-dependent processes. We also investigated whether a single exponential model was adequate to explain the dynamics of the metabolic light response in primates. Finally, we present a model that can explain why the speed of this transition in  $QO_2$  varies across species.

## Materials and Methods

### Animal Preparation

Experiments were performed in accordance with the ARVO Statement for the Use of Animals in Ophthalmic and Vision Research. We also obtained approval from our Institutional Animal Care and Use Committee. Five adult macaques (4 *Macaca fascicularis* (cynomolgus) and 1 *Macaca mulatta* (rhesus)) weighing 4 to 11 kg were used. The animals were from 11 to more than 25 years old, and had been used previously for skin tests of allergens. These are five of the six animals for which steady state aspects of retinal oxygenation have already been reported [4]; data of the type reported in this paper were not obtained from one rhesus monkey. Designations of the animals are the same in the two papers, where C indicates a cynomolgus and R indicates a rhesus. The methods for animal preparation and recording were reported previously [4,5,13,14]. Briefly, in anesthetized animals, two veins and a femoral artery were cannulated, and a tracheal tube was inserted for artificial ventilation following paralysis. Arterial blood pressure and blood gases were monitored via the arterial cannula. The two venous lines were used to deliver the anesthetic during surgery (pentothal) and a muscle relaxant (pancuronium bromide) during the experimental phase, and to control the blood glucose level at approximately  $100 \text{ mg-dl}^{-1}$  with infusions of insulin and glucose.

Following surgery on the eye, a 15-gauge needle was inserted to guide the double barreled oxygen microelectrode [15]. The pupil was dilated with 1% phenylephrine and 1% atropine topically. Flurbiprofen sodium ophthalmic solution (0.03%) was administered to block traumatic pupillary constriction [16,17]. During experiments the animal was anesthetized with a mixture of isoflurane (1 to 2%) and N<sub>2</sub>O:O<sub>2</sub> (0.70:0.30 to 0.75:0.25). After paralysis, arterial blood gas parameters were examined periodically with a blood gas analyzer (Model 860, Bayer Diagnostics, New York, USA), and were maintained within the normal range [4]. The body temperature was maintained at 39°C using a feedback-controlled heating blanket. Heart rate and arterial blood pressure were also monitored to evaluate the anesthesia.

### Measuring Retinal PO<sub>2</sub> Responses to Light

Double-barreled PO<sub>2</sub> microelectrodes were used to record retinal PO<sub>2</sub> changes induced by illumination. The microelectrode was positioned in or near the inner segment layer in the outer retina, where the PO<sub>2</sub> reached a minimum during dark adaptation. Baseline PO<sub>2</sub> was recorded for 30 seconds in darkness before a light stimulus was delivered, and then during and after 2 minutes of diffuse illumination at 0 to 4.0 log units of attenuation from the maximum, which was 11.5 log quanta (555 nm)-deg<sup>-2</sup>-sec<sup>-1</sup>. The transients presented here were recorded in the perifoveal retina. The parafovea is defined to be a 0.5 mm wide annular region outside the fovea, which is the central 1.5 mm diameter area, and the perifovea is defined to be a 1.5 mm wide annulus outside of the parafovea [18]. During recording, we could not precisely determine whether the electrode was in the parafovea or perifovea, so the term designating the larger area, perifovea, is used here.

### Modeling Light-Evoked PO<sub>2</sub> Responses

An example of the change in PO<sub>2</sub> in response to two minutes of illumination is shown in Figure 1. The solid line superimposed on the data shows a single exponential fit. The time dependent PO<sub>2</sub> change was described by:

$$P = P_{\min} \quad 0 \leq t \leq t_d \quad (1)$$

$$P = P_{\min} + (P_{\max} - P_{\min}) (1 - \exp(-(t - t_d)/\tau)) \quad t \geq t_d \quad (2)$$

where  $t=0$  is the onset of light. In this model,  $P_{\min}$  is the baseline PO<sub>2</sub>, and  $P_{\max}$  is the maximum PO<sub>2</sub> at steady state during the light stimulus. The time delay  $t_d$  is the time between the onset of light and the initial change in PO<sub>2</sub>, and  $\tau$  is the time constant of the PO<sub>2</sub> change.  $P_{\min}$  was computed from the initial 30 seconds under dark adaptation, and  $t_d$ ,  $P_{\max}$  and  $\tau$  were fitted to achieve the minimum root mean squared error (rms). The maximum light-evoked PO<sub>2</sub> change is  $\Delta PO_2 = P_{\max} - P_{\min}$ , as shown in Figure 1.

For those illuminations in which the PO<sub>2</sub> returned to baseline during the time when data were being digitized by the computer, the time constant for recovery,  $\tau_{\text{off}}$ , was also obtained with an equation for a decreasing exponential starting at  $P_{\max}$ . In cases where there might be confusion, the time constant at the onset of light,  $\tau$ , is called  $\tau_{\text{on}}$ .

### Statistics

All values are reported as mean  $\pm$  standard deviation when the data were normally distributed; otherwise, median values are reported. Statistical significance was determined with Student's  $t$ -test or linear regression analysis and was defined as a  $p$ -value  $< 0.05$ .

## RESULTS

A typical set of individual PO<sub>2</sub> responses to illumination in the inner segment layer of the photoreceptors is illustrated in Figure 2 (Monkey C4). The illumination that produced these responses varied between 7.5–10.5 log quanta (555 nm)-deg<sup>-2</sup>-sec<sup>-1</sup>, as shown at the right of the figure. The bold lines superimposed on the data show the fit of the single exponential function. We chose to position the electrode and to collect the data in the inner segment layer because this is where the photoreceptor oxygen consumption (QO<sub>2</sub>) occurs [19], and where the light-evoked PO<sub>2</sub> change is maximal.

At all illuminations, PO<sub>2</sub> increased at the onset of light, and then decreased when the light was turned off. At lower illuminations, 7.5 and 8.5 log quanta (555 nm)-deg<sup>-2</sup>-sec<sup>-1</sup>, the PO<sub>2</sub> returned to the baseline 30–60 seconds after the light was turned off. However, at higher illuminations, the PO<sub>2</sub> only partially recovered with a rapid time course. It then gradually decreased, and took more than 15 min after the offset of the stimulus to recover. Before giving another stimulus, we waited until the PO<sub>2</sub> had nearly fully recovered.

Figure 3 shows the magnitude of the light-evoked change in PO<sub>2</sub> ( $\Delta$ PO<sub>2</sub>) as a function of illumination in all five monkeys. Plots for each monkey are normalized to the maximum value of  $\Delta$ PO<sub>2</sub> in that animal. The  $\Delta$ PO<sub>2</sub> increased linearly with log illumination to a maximum over the lower part of the illumination range, and then, as in the example of Figure 2, decreased somewhat at the highest illumination in all animals. The illumination at which the maximum occurred was 8.5 log quanta (555 nm)-deg<sup>-2</sup>-sec<sup>-1</sup> in one animal, 9.5 log quanta (555 nm)-deg<sup>-2</sup>-sec<sup>-1</sup> in three animals, and 10.5 log quanta (555 nm)-deg<sup>-2</sup>-sec<sup>-1</sup> in one.

As illustrated in Figures 1 and 2, a single exponential equation was adequate to fit all the transients in the five monkeys, characterized by small rms errors between 0.26 and 2.54 mm Hg. The time constant varied from 14 to 120 seconds with a median of 26.0 seconds, and was not normally distributed (Figure 4A). A similar distribution was found in the cat [20]. In the monkey retina, most time constants fell between 15–50 seconds, except for two exceptionally high values (91.75 and 120.26 sec) in monkey C1. The quality of the fit to these two transients was good (rms error = 1.18 and 0.58), and the reason for the long  $\tau$  is unknown.

Figure 4B shows  $\tau$  as a function of illumination. A linear regression of the dependence of  $\tau$  on illumination was done for each animal and had a slope significantly different from zero only in monkeys C1 and R2 ( $p=0.02, 0.01$ ). In these animals,  $\tau$  decreased with increasing illumination. Note that monkey C1 also was the most different in Figure 3, and its data should probably be considered atypical. Monkey R2 was older than any cynomolgus monkey, at more than 25 years, but all the cynomolgus were approximately the same age (10 to 13 years), so age was probably not a factor. There was no significant dependence of  $\tau$  on illumination across all animals.

The time delay,  $t_d$ , for the five animals was  $4.6 \pm 1.3$  seconds (mean  $\pm$  SEM) and was significantly different from zero ( $p = 0.026, n=5$ ).

When the oxygen response recovered rapidly, as illustrated by the responses at lower illuminations in Figure 2, it was possible to fit a single exponential function to the recovery (off response), and the fitting error was equally small for both the on and the off responses. The median  $\tau_{\text{off}}$  was 20.7 sec, similar to the time constant for the response at the onset of illumination. For responses where both time constants were available, there was no correlation between the time constant for the increase in PO<sub>2</sub> ( $\tau_{\text{on}}$ ) and the decrease in PO<sub>2</sub> ( $\tau_{\text{off}}$ ) after an outlier was excluded from the analysis ( $p=0.78, n=14$ ). The correlation between  $\tau_{\text{off}}$  and illumination was also analyzed, and was not significant ( $p=0.46, n=14$ ).

## DISCUSSION

### Light evoked PO<sub>2</sub> responses

At all illuminations tested in the monkey retina, light evoked an increase in PO<sub>2</sub> in the inner segment layer of the photoreceptors, indicating that QO<sub>2</sub> decreased. A similar change has been observed in all other vertebrate retinas examined [1–3,6,8,21]. The size of the change in QO<sub>2</sub> cannot be determined from the light responses presented here, but fitting of a model to oxygen profiles allowed us to conclude that strong illumination decreased QO<sub>2</sub> to 72% of the dark-adapted level [4].

We were interested to know how the illumination required for the metabolic change corresponded to that required for electrical responses of rods, which has never been analyzed before. Figure 3 shows a rough extrapolation of the PO<sub>2</sub> vs. illumination function to an illumination that would cause a change in PO<sub>2</sub> that is 10% of the maximum. We can view this as a “metabolic threshold” illumination of about 6.6 log quanta (555 nm)-deg<sup>-2</sup>-sec<sup>-1</sup> (i.e., 4 x 10<sup>6</sup> quanta (555 nm)-deg<sup>-2</sup>-sec<sup>-1</sup>) at the cornea. It can be shown theoretically, using a three layer model of outer retinal oxygenation [19], that the amplitude of the PO<sub>2</sub> increase is linearly related to the amplitude of the QO<sub>2</sub> decrease, so this is also the illumination at which QO<sub>2</sub> is reduced by 10% from the dark-adapted maximum. The question is how this corresponds to the illumination required for electrical responses of photoreceptors. It is possible to calculate the fraction of the cyclic nucleotide-gated light-dependent channels that must be closed at this illumination, and therefore the fraction of the rod’s current response, in the following way. Assuming 1) that rhesus and human values are similar, 2) that there are approximately 3.3 degrees-mm<sup>-1</sup> on the human retina ([22], p. 96), 3) that the perifoveal density of rods is approximately 1.4 x 10<sup>5</sup> rods-mm<sup>-2</sup> in humans [23], and 4) that approximately 10% of the incident quanta are absorbed by human rods [24], then 4 x 10<sup>6</sup> quanta (555 nm)-deg<sup>-2</sup>-sec<sup>-1</sup>, the metabolic threshold, corresponds to an absorption of about 31 quanta-rod<sup>-1</sup>-sec<sup>-1</sup>. Data on the fractional reduction in inward cation current for individual mammalian rods as a function of steps of illumination as long as 15 sec are provided by Tamura, et al. [25] for cat, and Kraft, et al. [26] for human. The current responses reach a plateau at this stimulus duration, and are likely to represent the situation for the longer periods of illumination used in the present work. We have fitted these data with the function  $r/r_{\max} = 1 - \exp(-k_s I)$ , where  $r$  is the current,  $r_{\max}$  is the maximum inward current (dark current),  $k_s$  is a constant, and  $I$  is illumination [25,26]. The fits (which were not done in the original papers) are good overall, but not at the low illuminations relevant here. A separate linear fit or polynomial fit is much better for both human and cat. For human data, the polynomial fit for  $I < 200$  quanta (absorbed)-rod<sup>-1</sup>-sec<sup>-1</sup> is  $r/r_{\max} = -8.7 \times 10^{-6} (I)^2 + 2.97 \times 10^{-3} (I)$ . At 31 quanta-rod<sup>-1</sup>-sec<sup>-1</sup>,  $r/r_{\max}$  is 0.084. That is, oxygen consumption changes by about 10% at an illumination that closes 8.4% of the open channels. This calculation mixes photoreceptor data from isolated human rods and oxygen data from intact primate retina and may have other approximations, but a corresponding calculation for cat oxygen data from Figure 5 of Linsenmeier [3] and cat photoreceptor data [25] give a similar relationship. In cat, about 13% of the channels are closed when  $Q$  changes by 10%. The similarity between the metabolic change and the current change is a new result, but is not surprising, because channel closure reduces sodium inflow, which in turn reduces the energetically demanding pumping of sodium.

The “metabolic threshold” illumination is relatively weak in that it does not cause much light adaptation even if applied continuously [25,26], but it is not near the threshold of vision. The metabolic threshold illumination (more conveniently expressed as 4 x 10<sup>6</sup> quanta (555 nm)-deg<sup>-2</sup>-sec<sup>-1</sup>) is more than five log units above the human absolute visual threshold of 23 quanta-deg<sup>-2</sup>-sec<sup>-1</sup> [27], so over these several log units of illumination, rod metabolism is essentially the same as it is in the dark. This difference between metabolic threshold and absolute visual threshold occurs because near visual threshold very few channels are closed per rod.

The normalized  $PO_2$  change increased with illumination until the illumination reached a certain level, and then started to decrease, a phenomenon that was not observed in cat [3]. It is possible that the retina had not fully recovered before the highest illumination was used, resulting in a smaller response at the highest illumination, but an effort was made to wait for full recovery of the  $PO_2$  after each stimulus. The increase and then decrease of  $\Delta PO_2$  may be attributable to the way in which the two underlying metabolic processes,  $Na^+ /K^+$  pumping and cGMP turnover, change with illumination. At the onset of illumination, some fraction of the cyclic nucleotide gated channels close, causing a smaller influx of  $Na^+$ , a reduction of the workload of the  $Na^+ /K^+$  pump, as noted above, and a resulting decrease in  $QO_2$ . The cGMP turnover rate increases during illumination [10,28], causing an increase in  $QO_2$  [6]. The  $PO_2$  change at all illuminations reflects the sum of these two processes, which, unfortunately, cannot be separated from each other in monkey or cat, because only one time constant is needed to fit the data. With increasing illumination, the decrease of  $QO_2$  due to the closure of the channels is expected to saturate when all the channels are closed, but the cGMP contribution may continue to grow. This would lead to a smaller net decrease in  $QO_2$  and therefore a smaller  $\Delta PO_2$  at the highest illuminations. The smaller change in  $QO_2$  during illumination in monkey than in cat [4], could also be a reflection of a different balance between the two processes in different species.

The illumination at which the largest response was observed varied somewhat from animal to animal. The reason for this variation is unknown, but we speculate that this was largely due to experimental error. The distance between the light source and the cornea may have been somewhat different in different animals and some of the older animals had partial cataracts. It is also possible that the electrode was not in exactly the same location with respect to the inner segments during all stimuli in an animal. If the electrode started in the location of the maximum amplitude of the light-evoked change, which occurs approximately where the  $PO_2$  is lowest in the dark in the inner segment layer, any movement of the electrode relative to the retina during the long recording period required to obtain an intensity series would position the electrode at a point on the oxygen gradient where the  $\Delta PO_2$  would be smaller. Electrode movement is expected to have only a small effect, however, based on simulations of the light- and dark-adapted profiles. The light-evoked change is expected to decrease by 2 mm Hg or less as the electrode moves  $\pm 15 \mu m$  away from the location of the maximum  $\Delta PO_2$ , so we do not think that it can account for the decrease in  $\Delta PO_2$  at high illumination. The influence of electrode position on  $\Delta PO_2$  can be appreciated by inspection of actual or theoretical oxygen profiles [3,19,29]. (A change in position would not affect  $\tau$  either, as noted below.)

### Recovery from illumination

After the light was turned off, the  $PO_2$  recovered. At lower illuminations, such as 7.5 and 8.5 log quanta (555 nm)-deg<sup>-2</sup>-sec<sup>-1</sup>,  $PO_2$  returned to baseline shortly after the light was turned off; but at higher illuminations, >8.9 log quanta (555 nm)-deg<sup>-2</sup>-sec<sup>-1</sup>, the recovery was very slow. In some cases reestablishing the baseline took more than 10 minutes after the end of illumination. The slow recovery is evidence of the rod aftereffect that occurs above rod saturation, which can be observed in horizontal cells [30], and RPE cells [31]. A metabolic rod aftereffect has been observed previously in  $PO_2$  recordings from cat [3] and indicates that oxygen consumption continues to be suppressed while the membrane potential is hyperpolarized.

### Dynamics of $PO_2$ changes

Fitting the light-evoked  $PO_2$  responses with an exponential was a means of quantifying the time course of the change in photoreceptor  $QO_2$ . Some justification is needed for the contention that  $\tau$  for the  $QO_2$  change is the same as  $\tau$  that was measured for the  $PO_2$  change. The time course of the measured  $PO_2$  change at a point in the retina will depend on two factors: the speed

of the change in  $QO_2$  at that location, and diffusion from the source of  $O_2$  when the  $PO_2$  in the inner segment layer is altered by the  $QO_2$  change (i.e., readjustment of the gradients). The time constant for the oxygen to diffuse from the choroid to the inner segments is given approximately by  $L^2/D$ , where  $L$  is the distance from the choroid to middle of the inner segments, about 30  $\mu\text{m}$ , and  $D$  is the diffusion coefficient for oxygen in the retina, about  $2 \times 10^{-5} \text{ cm}^2/\text{sec}$  [32]. This diffusion time constant is about 0.5 seconds, which is much shorter than the measured  $\tau$  (26.0 seconds), indicating that the time course of the change in  $PO_2$  is dominated by the change in photoreceptor  $QO_2$  rather than by diffusion, and also that slight changes in electrode position would not affect  $\tau$ .

In monkey, a single exponential was adequate to fit the data, and the most parsimonious explanation is that the two metabolic processes that change with light, cGMP synthesis and  $Na^+$  pumping, have similar dynamics. However, it may also be possible to fit the data with a double exponential [6], in which the values of  $\tau$  for the two processes are somewhat different, and this needs to be considered. To address this possibility, a simulation was done in order to determine how different the dynamics of the two processes could be, and still fit the oxygen transients as well as the single exponentials reported in the results. The double exponential has 6 parameters, but several constraints can be imposed. First, in both toad and rabbit, where the two processes have been separated pharmacologically, the  $PO_2$  change caused by the  $Na^+$ -dependent process is about three times larger in amplitude as the cGMP dependent process, and in the opposite direction. Second, if there are two different values of  $\tau$ , the cGMP process is expected to be faster, as it is in toad. Third, it was assumed that  $t_d$  in the two processes is the same, because this gives an upper bound on the amount by which the two values of  $\tau$  could differ and still fit the data. The analysis showed that the maximum difference in the two time constants of a double exponential model compatible with a good fit was about 8 sec, which occurred when the slower  $\tau$  was 22 sec and the faster  $\tau$  was 14 sec (compared to the single  $\tau$  of 26 sec). Any reduction in the slower  $\tau$  below 22 sec did not yield a good fit for any value of the faster  $\tau$ , and neither did an increase in the slower  $\tau$  above 26 sec. Thus, a model in which there are two time constants differing by as much as about 8 sec is also compatible with the data. It will not be possible to characterize the dynamics further until techniques are available for isolating each component in primate retina.

### Comparison among species

The time constant found here for monkeys, with a median of 26 seconds, is considerably longer than the 10–13 seconds in cat [11], a little longer than the 21 sec (reported as a half time of 15 sec) in rat [12], and shorter than the 50.5 sec (reported as a half time of 35 sec) in rabbit [8]. There are other data on light-dark transitions in rabbit [33] and monkey [34] that show slower responses, but the measurements were made in the vitreous, where the distance to the inner segments is long enough that diffusion influences the time constant. In the toad retina, a double exponential model with two time constants was needed at high illumination, while at dim illumination, a single exponential equation was adequate [6]. The time constants in the toad were 60 and 180 seconds [6], with the faster time constant corresponding to the cGMP process and the longer time constant corresponding to the  $Na^+$ -dependent process that increases  $PO_2$ , as in cat and monkey. For technical reasons, the best fitting time constant for toad may be an overestimate [6]. Another estimate of the time constant for slowing the  $Na^+/K^+$  pump during illumination, derived from fitting potassium data to a model, was 110 to 170 sec [35]. These interspecies differences in the metabolic time constants can be at least partially explained by a model in which intracellular  $Na^+$  is the important parameter.

Intracellular  $Na^+$  concentration ( $[Na^+]_i$ ) is well known to control the rate of  $Na^+$  pumping in many cells [36], including rods [7]. If  $[Na^+]_i$  is mainly responsible for the change in  $Na^+$  pumping, and in turn for the time constant of  $QO_2$  and  $PO_2$ , then the differences among animals

may be related to the way in which  $\text{Na}^+$  influx influences  $[\text{Na}^+]_i$ . The  $\text{Na}^+$  influx is about the same across dark-adapted mammals, based on the similarity of the maximum dark current, which is 25 to 35 pA [37,38] in the species where this has been measured. Because in the dark-adapted steady state all the  $\text{Na}^+$  that enters the cell must leave it via the pump, the similarity of dark current means that individual rods in each animal must have approximately the same pumping rate in the dark. (Part of the dark current is due to  $\text{Ca}^{+2}$ , but because this is eliminated by an exchange for  $\text{Na}^+$ ,  $\text{Ca}^{+2}$  influx just leads to an additional influx of  $\text{Na}^+$ .) As light is absorbed by each photoreceptor, cation channels close. If a given fraction of the channels close, the  $\text{Na}^+$  influx will decrease by that same fraction. The rate at which a change in flux will affect  $[\text{Na}^+]_i$  should then be proportional to the initial pool of  $\text{Na}^+$  inside the cell, i.e. to the volume of the photoreceptor. Because the lengths of outer segments are about the same in different animals [39,40], the time required for  $[\text{Na}^+]_i$  to decrease by some amount should be proportional to the cross-sectional area of the outer segment. The cross sectional area depends on the radius of rod outer segments (ROS) squared, and these radii in toad, macaque, cat and rat are about 1.9 – 2.4  $\mu\text{m}$  [40], 1  $\mu\text{m}$  [26,39], 0.65  $\mu\text{m}$  [25] and 0.7  $\mu\text{m}$  [41] respectively. Outer segment diameter varies with eccentricity in monkey [39] but not enough to affect the analysis.

The ROS in rabbits have a radius of about 0.75  $\mu\text{m}$ , based on statements or measurements from figures in several references [42–44]. However, unlike the other mammals, the rod inner segments (RIS) of rabbits are much larger than the ROS, with a radius of 1.58  $\mu\text{m}$  [45], so an average of RIS and ROS radii are used in the calculation for rabbits. Because of the presumed linkage between  $[\text{Na}^+]_i$ , pump rate,  $\text{QO}_2$ , and  $\text{PO}_2$ ,  $\text{PO}_2$  should increase with time at the same rate that  $[\text{Na}^+]_i$  decreases. The hypothesis is then that  $\tau$  for  $\text{PO}_2$  changes should depend on rod cross sectional area, or radius squared. Figure 5 shows that the variation in time constant across animals is well predicted by this hypothesis for the four mammals ( $R^2 = 0.87$ ), and even the toad data are compatible with this explanation, despite the lower metabolic rate in toad. Some caution is warranted because the dimensions used are from different studies than the time constants, and may not apply exactly to the regions where time constants were measured, and several approximations have been made. However, it appears that the rate at which  $\text{Na}^+$  influx changes the intracellular  $\text{Na}^+$  concentration could largely account for species differences in the rate at which photoreceptor metabolism is adjusted during illumination.

## Acknowledgments

Supported by NIH R01 EY05034. The authors thank Dr. Norbert D. Wangsa-Wirawan and Mrs Yun Kim for their help during experiments and Mr. Kurt Qing for assistance with analysis.

## References

1. Sickel, W. Retinal metabolism in dark and light. In: Fuortes, MGF., editor. Physiology of Photoreceptor Organs Handbook of Sensory Physiology. Berlin: Springer Verlag; 1972. p. 227-727.
2. Zuckerman R, Weiter JJ. Oxygen transport in the bullfrog retina. *Exp Eye Res* 1980;30:117–127. [PubMed: 6968271]
3. Linsenmeier RA. Effects of light and darkness on oxygen distribution and consumption in the cat retina. *J Gen Physiol* 1986;88:521–542. [PubMed: 3783124]
4. Birol G, Wang S, Budzynski E, Wangsa-Wirawan ND, Linsenmeier RA. Oxygen distribution and consumption in the macaque retina. *American journal of physiology* 2007;293:H1696–1704. [PubMed: 17557923]
5. Braun RD, Linsenmeier RA. Retinal oxygen tension and the electroretinogram during arterial occlusion in the cat. *Invest Ophthalmol Vis Sci* 1995;36:523–541. [PubMed: 7890484]
6. Haugh-Scheidt LM, Griff ER, Linsenmeier RA. Light-evoked oxygen responses in the isolated toad retina. *Exp Eye Res* 1995;61:73–81. [PubMed: 7556472]



7. Shimazaki H, Oakley B 2nd. Decline of electrogenic Na<sup>+</sup>/K<sup>+</sup> pump activity in rod photoreceptors during maintained illumination. *J Gen Physiol* 1986;87:633–647. [PubMed: 2422316]
8. Ames A, Li YY, Heher EG, Kimble CR. Energy metabolism of rabbit retina as related to function: high cost of Na transport. *J Neuroscience* 1992;12:840–853.
9. Kimble EA, Svoboda RA, Ostroy SE. Oxygen consumption and ATP changes of the vertebrate photoreceptor. *Exp Eye Res* 1980;31:271–288. [PubMed: 6968685]
10. Dawis SM, Graeff RM, Heyman RA, Walseth TF, Goldberg ND. Regulation of cyclic GMP metabolism in toad photoreceptors. Definition of the metabolic events subserving photoexcited and attenuated states. *J Biol Chem* 1988;263:8771–8785. [PubMed: 2837463]
11. Braun RD, Linsenmeier RA, Goldstick TK. Oxygen consumption in the inner and outer retina of the cat. *Invest Ophthalmol Vis Sci* 1995;36:542–554. [PubMed: 7890485]
12. Cringle SJ, Yu DY, Yu PK, Su EN. Intraretinal oxygen consumption in the rat in vivo. *Invest Ophthalmol Vis Sci* 2002;43:1922–1927. [PubMed: 12037000]
13. Padnick-Silver L, Linsenmeier RA. Effect of acute hyperglycemia on oxygen and oxidative metabolism in the intact cat retina. *Invest Ophthalmol Vis Sci* 2003;44:745–750. [PubMed: 12556408]
14. Wang S, Linsenmeier RA. Hyperoxia improves oxidative metabolism in the detached feline retina. *Invest Ophthalmol Visual Sci*. 2007 in press.
15. Linsenmeier RA, Yancey CM. Improved fabrication of double-barreled recessed cathode O<sub>2</sub> microelectrodes. *J Appl Physiol* 1987;63:2554–2557. [PubMed: 3436887]
16. van Haeringen NJ, van Sorge AA, Carballosa Core-Bodelier VM. Constitutive cyclooxygenase-1 and induced cyclooxygenase-2 in isolated human iris inhibited by S(+) flurbiprofen. *J Ocul Pharmacol Ther* 2000;16:353–361. [PubMed: 10977131]
17. Thaller VT, Kulshrestha MK, Bell K. The effect of pre-operative topical flurbiprofen or diclofenac on pupil dilatation. *Eye (London, England)* 2000;14 ( Pt 4):642–645.
18. Park, SS.; Sigelman, J.; Gragoudas, ES. The anatomy and cell biology of the retina. In: Tasman, W.; Jaeger, EA., editors. *Duane's Foundations of Clinical Ophthalmology*. Philadelphia: Lippincott-Raven; 1996.
19. Haugh LM, Linsenmeier RA, Goldstick TK. Mathematical models of the spatial distribution of retinal oxygen tension and consumption, including changes upon illumination. *Ann Biomed Eng* 1990;18:19–36. [PubMed: 2306030]
20. Chatters, TC. *Biomedical Engineering*. Evanston, Illinois: Northwestern University; 1988. An investigation of the light-evoked changes in oxygen consumption in the outer retina of the cat.
21. Winkler, BS. A quantitative assessment of glucose metabolism in the isolated rat retina. In: Christen, Y.; Doly, M.; Droy-Lefaix, M., et al., editors. *Les Seminaires ophthalmologiques d'IPSEN, Vision et adaptation*. Paris: Elsevier; 1995. p. 78-96.
22. Oyster, CW. *The Human Eye: Structure and Function*. Sunderland, MA: Sinauer Associates; 1999.
23. Wikler KC, Williams RW, Rakic P. Photoreceptor mosaic: number and distribution of rods and cones in the rhesus monkey retina. *The Journal of comparative neurology* 1990;297:499–508. [PubMed: 2384610]
24. Rushton WA. The rhodopsin density in the human rods. *The Journal of physiology* 1956;134:30–46. [PubMed: 13377310]
25. Tamura T, Nakatani K, Yau KW. Light adaptation in cat retinal rods. *Science* 1989;245:755–758. [PubMed: 2772634]
26. Kraft TW, Schneeweis DM, Schnapf JL. Visual transduction in human rod photoreceptors. *The Journal of physiology* 1993;464:747–765. [PubMed: 8229828]
27. Denton EJ, Pirenne MH. The absolute sensitivity and functional stability of the human eye. *The Journal of physiology* 1954;123:417–442. [PubMed: 13152690]
28. Ames A 3rd, Walseth TF, Heyman RA, et al. Light-induced increases in cGMP metabolic flux correspond with electrical responses of photoreceptors. *J Biol Chem* 1986;261:13034–13042. [PubMed: 2875993]
29. Linsenmeier RA, Yancey CM. Effects of hyperoxia on the oxygen distribution in the intact cat retina. *Invest Ophthalmol Vis Sci* 1989;30:612–618. [PubMed: 2703302]

30. Steinberg RH. The rod after-effect in S-potentials from the cat retina. *Vision research* 1969;9:1345–1355. [PubMed: 5358839]
31. Schmidt R, Steinberg RH. Rod-dependent intracellular responses to light recorded from the pigment epithelium of the cat retina. *The Journal of physiology* 1971;217:71–91. [PubMed: 5571953]
32. Roh HD, Goldstick TK, Linsenmeier RA. Spatial variation of the local tissue oxygen diffusion coefficient measured in situ in the cat retina and cornea. *Advances in experimental medicine and biology* 1990;277:127–136. [PubMed: 2096618]
33. Tillis TN, Murray DL, Schmidt GJ, Weiter JJ. Preretinal oxygen changes in the rabbit under conditions of light and dark. *Invest Ophthalmol Vis Sci* 1988;29:988–991. [PubMed: 3372171]
34. Stefansson E, Wolbarsht ML, Landers MB 3rd. In vivo O<sub>2</sub> consumption in rhesus monkeys in light and dark. *Exp Eye Res* 1983;37:251–256. [PubMed: 6628573]
35. Shimazaki H, Oakley B 2nd. Reaccumulation of [K<sup>+</sup>]<sub>o</sub> in the toad retina during maintained illumination. *J Gen Physiol* 1984;84:475–504. [PubMed: 6090581]
36. Rossier BC, Geering K, Kraehenbuhl JP. Regulation of the sodium pump: how and why? *Trends in Biochemical Sciences* 1987;12:483–487.
37. Baylor DA, Lamb TD, Yau KW. The membrane current of single rod outer segments. *The Journal of physiology* 1979;288:589–611. [PubMed: 112242]
38. Baylor DA, Nunn BJ, Schnapf JL. The photocurrent, noise and spectral sensitivity of rods of the monkey *Macaca fascicularis*. *The Journal of physiology* 1984;357:575–607. [PubMed: 6512705]
39. Hoang QV, Linsenmeier RA, Chung CK, Curcio CA. Photoreceptor inner segments in monkey and human retina: mitochondrial density, optics, and regional variation. *Visual neuroscience* 2002;19:395–407. [PubMed: 12511073]
40. Zhang YD, Straznicky C. The morphology and distribution of photoreceptors in the retina of *Bufo marinus*. *Anatomy and embryology* 1991;183:97–104. [PubMed: 1905114]
41. Mayhew TM, Astle D. Photoreceptor number and outer segment disk membrane surface area in the retina of the rat: stereological data for whole organ and average photoreceptor cell. *Journal of neurocytology* 1997;26:53–61. [PubMed: 9154529]
42. Bunt AH. Fine structure and radioautography of rabbit photoreceptor cells. *Invest Ophthalmol Vis Sci* 1978;17:90–104. [PubMed: 624609]
43. Sjostrand, FS.; Nilsson, SE. The structure of the rabbit retina as revealed by electron microscopy. In: Prince, JH., editor. *The Rabbit in Eye Research*. Springfield, IL: Charles C. Thomas; 1964. p. 449–513.
44. Townes-Anderson E, Dacheux RF, Raviola E. Rod photoreceptors dissociated from the adult rabbit retina. *J Neurosci* 1988;8:320–331. [PubMed: 3339415]
45. Tucker GS, Hamasaki DI, Labbie A, Bradford N. Physiologic and anatomic development of the photoreceptors of normally-reared and dark-reared rabbits. *Experimentelle Hirnforschung* 1982;48:263–271.

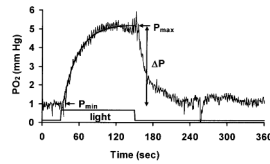


**Figure 1.**

An example of the change in  $PO_2$  in the distal retina during 2 min of illumination at  $8.5 \log$  quanta ( $555 \text{ nm}$ )- $\text{deg}^{-2}\text{-sec}^{-1}$ . The solid line superimposed on the data shows a single exponential equation fitted to the data. Light was on between  $t = 30$  and  $t = 150$  sec. In this example, the  $PO_2$  returned to baseline 90 sec after the light was turned off. Baseline  $PO_2$ , the maximum  $PO_2$  during illumination, and the difference between them are defined as  $P_{\min}$ ,  $P_{\max}$ , and  $\Delta PO_2$  respectively.

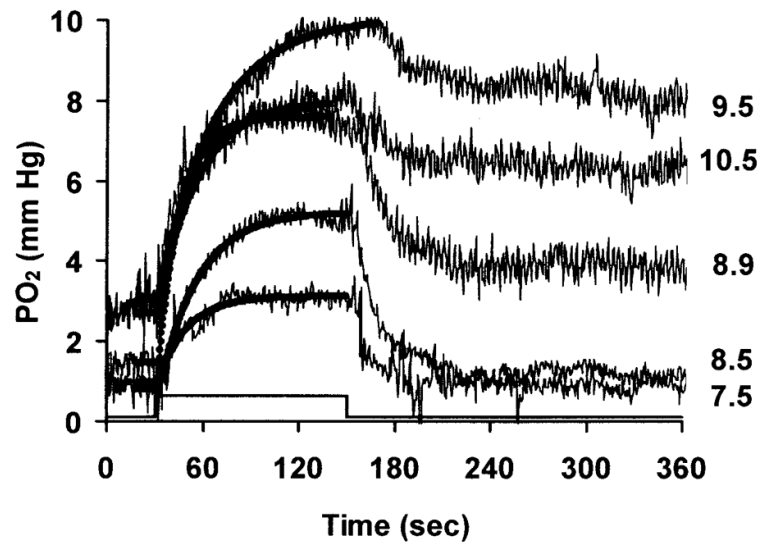


**Figure 2.**  $\text{PO}_2$  changes as a function of time during illumination in one monkey (C4). Each response corresponds to a single illumination, given in  $\log \text{quanta-deg}^{-2}\text{-sec}^{-1}$  at the right. Solid lines superimposed on the data show the single exponential fits. The light was on for 120 sec between 30 and 150 sec.

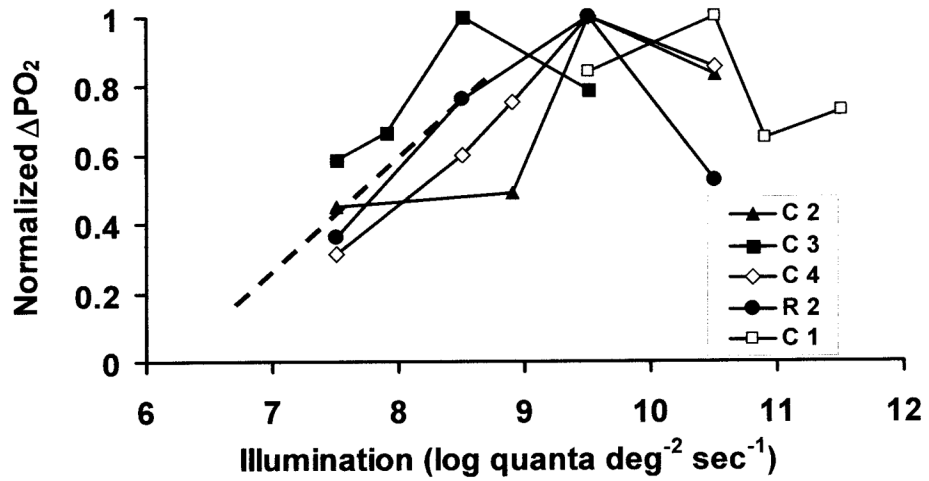


**Figure 3.**

The change in PO<sub>2</sub> (ΔPO<sub>2</sub>) as a function of illumination. Plots for each of five monkeys are normalized to the maximum value of ΔPO<sub>2</sub> in that animal. Each line represents a different monkey. The dashed line is a rough extrapolation to a small response at the “metabolic threshold” illumination, as described in the Discussion.

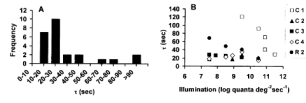


**Figure 4.**

(A) Frequency distribution of values of  $\tau$  at the onset of illumination across all responses. The median value was 26.0 seconds. (B) Time constant  $\tau$  as a function of illumination. The time constant was not significantly correlated with illumination in three monkeys, but was significantly correlated in monkeys C1 and R2 ( $p < 0.05$ ).

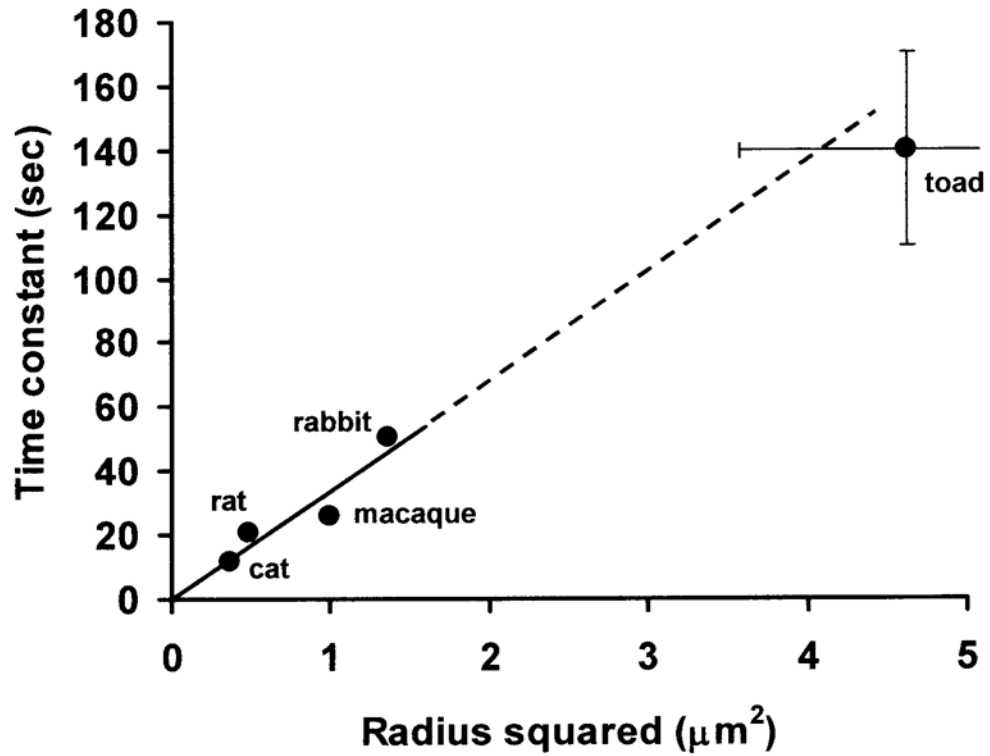


**Figure 5.**

The time constant of the  $\text{PO}_2$  response to light as a function of the square of rod photoreceptor radius for rat, rabbit, monkey, cat and toad. Outer segment radius was determined from direct measurements in previous studies as described in the text. For toad, the ranges given in the text are shown by the error bars (one is truncated so that the graph does not have to extend past  $5 \mu\text{m}^2$ ), and the circle is the mean. Ranges for the mammalian data are either unknown or are small. The solid line is a regression through the mammalian data only:  $\tau = 33.45 r^2 + 0.28$ , where  $r$  is in  $\mu\text{m}$  and  $\tau$  is in sec. ( $R^2 = 0.87$ .) The dashed line is an extension of this relationship to the toad data.